APPLICATION OF PROGNOSIS AND DIAGNOSIS TECHNIQUES OF ASR FOR A HISTORIC STRUCTURE

Anthony F. Bentivegna[1]*, Jason H. Ideker[2]

[1]CTLGroup, Skokie, IL, USA

[2]Private Consultant, Corvallis, OR, USA

Abstract

The Orchard Beach Bathhouse and promenade was a federally-funded public works project conceived during the Great Depression of the 1930s. Since its construction, the bathhouse has aged and suffered deterioration due to alkali-silica reaction (ASR), freeze-thaw cycling, and corrosion. The works summarized in this paper gives an overview of testing techniques for assessing the amount of deterioration due to ASR and the potential for continued deterioration. Over 400 cores were extracted from the historic concrete structure, although only a small subset will be reported in this paper. These cores were evaluated for typical mechanical properties and petrographic examination according to ASTM C856. In addition to these routine tests, damage rating index (DRI), stiffness damage testing (SDT), residual expansion testing, hot-water extraction of water soluble alkalis, and in-situ monitoring of crack propagation and expansion measurements were implemented on this structure. The findings of these techniques indicated the primary cause of deterioration was due to freeze-thaw deterioration and corrosion, although active ASR was observed.

Keywords: alkali-silica reaction, petrography, damage rating index, stiffness damage testing, water-soluble alkalis

1 INTRODUCTION

1.1 Background

The Orchard Beach Bathhouse and promenade (OBBH) was a federally-funded public works project conceived during the Great Depression of the 1930s. Located in Pelham Bay Park in the Bronx, New York and bordering the Long Island Sound, it was constructed in 1934-37. The public bathhouse served as the base for over 100,000 beachgoers during the summer months with a mile-long promenade, showers and locker rooms for 7,000 people, parking for 8,000 cars, restaurants, and is an aesthetically pleasing iconic concrete structure. Since its construction, the bathhouse has aged and suffered deterioration due to alkali-silica reaction (ASR), freeze-thaw cycling, and corrosion. Currently, the New York City Office of Parks, Recreation, and Historic Preservation Department and Mayor Bill de Blasio are interested in repurposing the structure, but needed to have an understanding of the potential for continued deterioration due to ASR.

OBBH is comprised of a mile long promenade and two main structures, the north and south loggia. Each loggia is a two story curving structure with concrete colonnades and embellished with blue terra-cotta tiles. Designed in a modern classical style, OBBH was constructed with a variety of materials including concrete, brick and limestone, along with tile and terrazzo. Both loggias are situated adjacent to the Pelham Bay which lies on the western end of the Long Island Sound. Being so, the structure is exposed to windborne and splash zone chloride particles, cyclic freezing and thawing conditions, and moisture from rain and snow. These environmental conditions, lack of maintenance, and materials concerns have left the structure in a questionable condition. Photographs of the existing conditions of the structure are shown in Figure 1.

1.2 Scope and Significance

Previously, a limited petrographic examination was performed, by others, and confirmed the presence of alkali-silica reaction (ASR) in a few concrete cores extracted from the precast coping beams. Due to this petrographic examination and the representative deterioration (i.e. map pattern cracking, efflioresce, staining), ASR was thought to be the primary cause of premature deterioration. The research team aimed to characterize the extent of damage due to ASR and other durability

* Correspondence to: abentivegna@ctlgroup.com

mechanisms, as well as determine the potential for continued deterioration due to ASR. Testing included evaluation of depth of chloride penetration, compressive strength testing, petrographic examination, damage rating index, residual expansion testing, stiffness damage testing, hot-water extraction of water-soluble alkalis, and in-situ monitoring of expansion and cracking of the structure. Due to the length of this paper not all results will be presented or discussed. This paper will be helpful for those interested in applying non-standardized techniques for determining the diagnosis and prognosis of structures, which suffer deterioration due to alkali-silica reaction.

2 MATERIALS AND METHODS

2.1 Materials

Over 400 (100 mm diameter) cores were extracted from OBBH. In this paper, only a part of the representative data obtained (cores from 10 locations of the structure) will be reported and discussed. These cores were wiped clean, placed in sealed plastic bags and shipped in protective sleeves for testing to a commercial testing laboratory in Skokie, Illinois, USA.

2.2 Methods for assessment and analysis

Petrographic Examination and Damage Rating Index (DRI)

Petrographic examination (ASTM C856) and DRI were performed on 57 cores. Petrographic examination was done to confirm consistency in the concrete's constituent materials throughout the structure and to identify distress mechanisms which might be contributing to the outward manifestations of damage (i.e. ASR, freeze-thaw deterioration, corrosion) [1].

Damage Rating Index (DRI) was performed to allow for a quantitative comparison of the conditions of the concrete cores. A plastic sheet with a 1-cm by 1-cm square grid was placed over the lapped surfaces from the petrographic examination. A concrete surface area of 200 cm² (200 squares) was evaluated. The gridded section was examined under a stereomicroscope at 16x magnification.

The DRI was evaluated for various features related to alkali-silica reaction (ASR) on each core. Features included but were not limited to air voids with ASR gel, cement paste with cracks, and debonded aggregate. Each feature was given a weighting factor based on the severity of damage associated with it. The features were all quantified within the gridded section of the core and then multiplied by the appropriate weighting factor. To get the final DRI, the weighted totals were normalized to represent a 100 cm² area. Table 1 summarizes the ASR features included in the analysis, the feature naming convention (used in the DRI sheets in the appendices), and the weighting factors. [2-8].

Residual Expansion Testing

The potential for further expansion due to ASR was determined using a testing procedure similar to ASTM C1293. Residual expansion testing was performed to evaluate the potential for continued expansion of the concrete cores. Cores were cut (100 mm by 300 mm), pinned at each end, and stored above water in a sealed 95 ± 5% RH container at 38°C and monitored for uniaxial length change and mass change [7, 9-12].

Stiffness Damage Testing

Stiffness damage testing (SDT) was done on cores from the structure to quantify and compare the extent of deterioration from around the different sections of the structure. SDT implements a cyclic, uniaxial compressive loading of concrete core samples (5 cycles). The reduction in the modulus of elasticity, the energy dissipated during the load-unload cycles, and the accumulation of plastic strain are used to characterize the amount of damage in the specimens. Cores were tested in similar moisture conditions to that which are present in the structure and were cut to 100 mm by 200 mm. The longitudinal deformation was measured using an unbonded compressometer with a linear variable differential transformer (LVDT). Specimens were loaded up to 10 MPa and unloaded to 0 MPa with a rate of loading and unloading of 0.1 $N/mm^2/s$ for 5 cycles [3, 7, 13-16].

Hot-water Extraction of Water-soluble Alkalis

The determination of the alkali content is useful for determining if there are sufficient alkalis to sustain ASR. Due to the age of the concrete (approximately 75 years) it would not be possible to extract sufficient pore solution for analysis; therefore, the alkali content was determined by using hot-water extraction method. This technique was used to determine the active- or water-soluble alkali content of the concrete on a kg/m^3 $Na_2O_{eq.}$ basis. A representative (approximately 2 kg) sample was crushed with a hammer to approximately 25 mm and allowed to dry. After drying, the concrete sample was progressively crushed and ground to pass the No. 100 sieve. Two 10 gram sub-samples were immersed in 100 mL of distilled water. The distilled water is boiled for 10 minutes and left to cool to room temperature overnight. The suspension was then filtered and sodium and potassium concentrations were determined by atomic absorption [7, 17].

In-situ Monitoring: Expansion and Crack Propagation

In addition to determining the prognosis of the structure via samples in the laboratory, in-situ monitoring of expansion, crack width opening and crack propagation of the concrete structure was initiated at 11 locations.

Expansion measurements were performed using a digital Mayes Gage Comparator. The comparator has a digital display with a precision of 0.001 mm. At each of the monitoring locations, four stainless steel gage pins were installed in the surface of the concrete in a 0.5 m x 0.5 m square pattern that allowed both vertical and horizontal measurements of expansion. The pins were inserted approximately 19 mm into the concrete surface and secured using a fast-setting epoxy; see Figure 2A and 2B. Four measurements are taken along the perimeter of the inspection area. The concrete surface temperature at the time of each measurement was recorded using an infrared thermometer in order to account for thermal expansion of the concrete [7,18-20].

Monitoring of the cracks and crack propagation was completed using a modified version of the cracking index. At each monitoring location a 0.5 m x 0.5 m square grid was drawn using the gage studs for the expansion measurements as reference points. Each side of the grid and the diagonals were divided into 0.1 m segments. For each segment, the number of cracks crossing the grid and their widths were recorded. Plastic crack comparator cards were used in combination with a handheld eye loupe to measure the crack widths. The data was used to calculate a Cracking Index (CI) for each location, based on the average total crack width per meter of the grid axis. The progression of alkali-silica reaction (ASR) in the structure should be reflected in an increase of the CI over time. The crack propagation measurement pattern and example monitoring are shown in Figure 2C and Figure 2D [7, 18, 20, 21].

3 RESULTS

Due to the amount of data from this testing, only data from the beam and columns of the two loggias (North Loggia and South Loggia) will be reported in this paper. In addition to the beams and columns, testing on the pile caps, slabs, copping beams, and foundation walls was also evaluated and a summary of the findings will be discussed in a later journal article. The naming convention used for the remainder of this report is: "NL" for North Loggia, "SL" for South Loggia and "B" for Beam, and "C" Column.

3.1 Petrography and DRI (Diagnosis)

Generally, from the petrographic examination, the cores were composed of concrete with similar constituent materials. The general composition of the concrete is summarized below:

- Portland cement paste - The paste contains residual portland cement clinker grains. The hardness of the paste varies from core to core, from soft to hard. Depth of paste carbonation is generally shallow, although deeper in several cores. The paste-aggregate bond varies from core to core, from weak to tight. In general, cores with weaker bonds are those with at least a moderate amount of deterioration.
- Siliceous aggregate – Similar aggregates were observed in all cores. The coarse aggregate is a natural gravel composed of a variety of rock types, generally including metaquartz, quartzite, and gneiss, with several particles of other various rocks. The particles are rounded to subangular in shape and are generally hard. The fine aggregate is mainly a quartz and metaquartz sand, with several particles of rocks and minerals similar to that in the coarse aggregate. Alkali-silica reaction (ASR) has occurred in some of the cores, while it was not observed in other cores. The reaction appeared to occur with the metamorphosed quartz in the aggregates.
- Air-void system and freeze-thaw deterioration - The concrete in all the cores is not air-entrained. Freeze-thaw deterioration is present in some of the cores; some of the deterioration is fairly extensive.
- ASR deterioration - ASR deterioration is generally present in conjunction when another type of deterioration is present, such as freeze-thaw. Therefore, the exact amount of ASR-related deterioration generally was difficult to discern. However, when present, the ASR

deterioration is generally minor, although it is present in greater amounts in several cores. ASR gel is present in some cores with no associated deterioration observed.

The normalized DRI values varied widely within the loggia and within the different elements of the loggia. The DRIs for the beams and columns varied from 7 to 427. A summary of the results for both loggias is shown in Figure 4.

Four cores (NL-B-1.2, NL-B-2.3, SL-B-1.2, and SL-B-2.3) from four beams were examined. The two cores from the North Loggia had little to no significant damage with DRIs of 31 and 15 for cores NL-B-2.3 and NL-B-1.2, respectively. These cores had minor amounts of damage with indications of reaction rims forming around particular coarse aggregate particles and a few randomly-oriented, hairline microcracks, extending into aggregate particles. Damage in these cores was substantially less than the damage observed in the cores from the South Loggia beams. Cores (SL-B-2.3 and SL-B-1.2) from the South Loggia beams had DRIs of 319 and 427, respectively. Both cores had numerous micro cracks and cracks. The cracks tended to be parallel to core end surfaces, passing through many coarse aggregate particles. Deposits of ettringite and ASR gel were observed throughout the core, especially filling air voids, cracks, and microcracks.

Six cores (NL-C-2, NL-C-3, NL-C-4, SL-C-2, SL-C-3, and SL-C-4) were examined from the upper end of the loggia columns. Cores NL-C-2, NL-C-3, NL-C-4 from the North Loggia had DRIs of 18, 7, and 15, respectively. In common, ASR gel filled many of the air voids and deposits of ettringite were observed lining cracks. Significant deterioration was observed in the three cores extracted from the upper column from the South Loggia. SL-C-2, SL-C-3, and SL-C-4 had DRIs of 237, 54, and 156, respectively. ASR gel deposits were common coating coarse aggregate and filling many air voids throughout the cores, and white secondary deposits fill many cracks and microcracks; deposits consist of ettringite, ASR gel, and calcium carbonate.

3.2 Stiffness damage testing (Diagnosis)

Results of the SDT are shown in Table 2. Six cores (NL-C-2, NL-C-3, NL-C-4, SL-C-2, SL-C-3, and SL-C-4) from the columns were evaluated. Significant more damage was observed with the total energy dissipated in all three cores from the South Loggia versus the North Loggia. However, Core NL-C-2 does have similar amount of energy dissipated in the first load/unload cycle as there appears to be from the South Loggia this core appears to be an outlier from the other two from the North Loggia. This trend in the data is reflected in the data from cores from the beams. The cores from South Loggia had an average energy dissipation 54% greater than the energy dissipated from the cores from the North Loggia.

3.3 Residual expansion testing (Prognosis)

The average expansion of two cores for each of the locations is summarized in Table 3, except for coring location NL-B-1.2 and NL-B-2.3 where cores of sufficient length for residual expansion testing could not be extracted. Residual expansion testing results for all cores ranged from 0.024-0.064%. According to Fournier et. al, this would indicate a high to very high potential for continued expansion due to ASR [7]. Results indicate a high potential for continued expansion in the cores from the columns versus cores extracted from the beams from both the North and South Loggia. The average expansion of cores from the columns in South and North Loggia is 43% and 46% greater than those from the beams, respectively.

3.4 Hot-water extraction water-soluble alkalis (Prognosis)

Results of the hot-water extraction of water-soluble alkalis are shown in Table 4. In all, but one of the cores evaluated from the beams and columns the concrete cores had alkali content greater than 2.3 kg/m^3. This indicates that enough alkali is present in the concrete to provide a source of alkalis for alkali-silica reaction to be sustained. In many of the cores the alkali content exceeds 3-3.6 kg/m^3 and this represents conditions that are highly favourable for alkali-silica reaction to occur given the potential for and existing alkali-silica reaction already observed in the structure.

3.5 In-situ Monitoring: Expansion and Crack Propagation (Prognosis)

At this time, the structure has been monitored for the first year after instrumentation. There has not been sufficient data collected to make any observations with the rate of deterioration or expansion of the structure. Results of the initial cracking propagation monitoring and CI are shown in Table 5. Average CI of the north loggia and south loggia is 2.5 and 1.5, respectively. This would classify the surface deterioration of the South Loggia as significant and the North Loggia moderate based on the initial CI. The authors have encouraged the owners to monitor the structure multiple times per year for the 5-10 years to get a better understanding on the rate of expansion and cracking.

4 DISCUSSION

Through the combination of the various diagnosis and prognosis testing techniques this paper has identified the cause of deterioration to be occurring due to ASR and cyclic freeze/thaw deterioration. Petrographic examination was used to identify the cause of deterioration, and that the concrete contains constituent materials known to be alkali-silica reactive. DRI and SDT confirmed areas of significant deterioration in the structure. The amount of deterioration varied drastically from North to South Loggia and within the elements of the same structure. These levels of deterioration are likely due to exposure conditions on the site. Concrete exposed to more moisture and winds appear to suffer the worst deterioration. Furthermore, concrete in the roof slabs, where drainage is poor, showed the most extensive damage from freeze-thaw attack and also contributions from ASR. Interior concrete from the structure showed very low levels of ASR related deterioration (e.g. reaction rims only with little no microcracking) and no freeze-thaw damage. However, this concrete showed the highest depths of carbonation, so the owners were cautioned to monitor carbonation depth of the future lifespan of the structure.

Stiffness damage testing (SDT) was implemented to quantify the extent of deterioration in concrete cores. It should be noted, the data was not used to estimate the amount of expansion which had occurred in the reinforced concrete structure. There was not sufficient information available on the concrete mixture proportions and constituents for the authors to develop a reliable expansion calibration curve. The significance of this data is to contribute to the quantification of the deterioration amongst the various structures and elements within the structures. The most effective ways thought to compare the amount of deterioration were through the energy dissipated in the first load/unload cycle and the accumulation of plastic strain through the five load/unload cycles where more energy dissipated and more plastic strain would indicate a core which has suffered from more deterioration.

The use of hot-water extraction of the water-soluble alkalis and residual expansion testing were used to determine the prognosis of the structure. Results from the hot-water extraction of the water-soluble alkalis showed that all the concrete cores had a high-to-very high potential for continued expansion due to the amount of available alkalis remaining in the concrete. The residual expansion testing results also indicated a high-to-very high potential for continued ASR.

From the results of all the testing, it is apparent the structure is suffering deterioration due ASR and cyclic freeze/thaw deterioration. It is hypothesized the concrete is cracking due to freeze/thaw and the cracks are serving as an avenue to allow moisture to enter the concrete for ASR to continue. The rate of expected deterioration is unknown at this time, but the authors recommend continuing to monitor the structure for expansion and crack propagation to help better assess the remaining service life.

5 CONCLUSIONS

This paper only purports a subset of the data produced from the characterization and testing of the 417 cores extracted from OBBH. This project represents the largest application of these various test methods aimed to determine the diagnosis, quantification of deterioration, and prognosis related to ASR. Combining the various test methods allowed the materials consultants, structural engineers, architects, historians and owners make educated decisions on the future use of the building due to the better understanding of the potential for continued deterioration due to ASR. This testing campaign highlighted that ASR was not the only active deterioration mechanism, and in fact freeze-thaw damage, corrosion of reinforcing steel and carbonation of the concrete are other contributing and often more severe than the ASR in the structure. Such a testing campaign is recommended for any historic or long-life structure where deterioration mechanisms are observed visually. OBBH has stood for 75 years it has suffered deterioration due to concrete constituents, environmental conditions, and lack of maintenance.

6 REFERENCES

[1] American Standards for Testing and Materials, "Standard Practice for Petrograpic Examination of Hardened Concrete," ASTM International, ASTM C856-11, Annual Book of ASTM Standards

[2] Smaoui, N., Berube, M.A., Fournier, B., Bissonnette, B., and Durand, B., "Evaluation of the expansion attained to date by concrete affected by alkali-silica reaction. Part 1: Experimental Study," 12th International Conference on AAR, Beijing (China), pp. 821-832, 2004.

[3] Smaoui, N., Berube, M.A., Fournier, B., Bissonnette, B., and Durand, B., "Evaluation of the expansion attained to date by concrete affected by alkali-silica reaction. Part III Application to Existing Structures.“ Canadian Journal of Civil Engineering. 32" 463-479, 2005

[4] Rivard, P., Fournier, B. and Ballivy, G., "The Damage Rating Index Method for ASR Affected Concrete– A Critical review of Petrographic Features of Deterioration and Evaluation Criteria," Cement, Concrete & Aggregates, Vol. 24, No. 2, pp. 1-11, 2002.

[5] Rivard, P., Fournier, B. and Ballivy, G., "Quantitative Petrographic Technique for Concrete Damage Due to ASR: Experimental and Application," Cement, Concrete & Aggregates, Vol. 22, No. 1, pp. 63-72, 2000.

[6] Shrimer, F.H., "Application and Use of Damage Rating Index in Assessment of AAR-Affected Concrete – Selected Case Studies," Proceedings of the 11th International Conference on Alkali-Aggregate Reaction in Concrete, Quebec City, Canada, Editors : M.A. Bérubé, B. Fournier and B.Durand, pp. 899-908, 2000.

[7] Fournier, B., Berube, M.A., Folliard, K.J., and Thomas, M.D.A, "Report on the Diagnosis, Prognosis, and Mitigation of Alkali-Silica Reaction (ASR) in Transportation Structures," Federal Highway Admistration, January 2010

[8] Villeneuve, V., Fournier, B., and Duchesne, J., "Determination of the damage in concrete affected by ASR – the Damage Rating Index (DRI), ICAAR 2012, Austin, Texas

[9] American Standards for Testing and Materials, "Standard Test Method for Determination of Length Change of Concrete Due to Alkali-Silica Reaction," ASTM International, ASTM C1293-08, Annual Book of ASTM Standards

[10] Berube, M.A., Smaoui, N. Cote, T., "Expansion Tests on Cores from ASR-Affected Structures," 12th International Conference on AAR, Beijing (China), pp. 821-832, 2004.

[11] Stark, D. and G. DePuy, "Alkali-Silica Reaction in Five Dams in Southwestern United States," American Concrete Institute Special Publication, pp. 1759-1786

[12] Fecteau, P.L. and Fournier, B., "Residual Expansion Testing: New Aspects on Cores Extracted from Exposure Blocks Submitted to Natural Environmental Conditions," ICAAR 2012, Austin, Texas

[13] American Standards for Testing and Materials, "Standard Test Method for Static Modulus of Elasticity and Poisson's Ratio of Concrete in Compression," ASTM International, ASTM C469-10, Annual Book of ASTM Standards

[14] American Standards for Testing and Materials, "Standard Test Method for Compressive Strength of Cylindrical Concrete Specimens," ASTM International, ASTM C39-12, Annual Book of ASTM Standards

[15] Giannini, E.," Evaluation of Concrete Structures Affected by Alkali-Silica Reaction and Delayed Ettringite Formation," The University of Texas at Austin, Ph.D. Dissertation, 2012

[16] Sanchez, L., Fournier, B., and Jolin, M., "Study of the parameters of the stiffness damage test for assessing concrete damage due to alkali-silica reaction (ASR)," ICAAR 2012, Austin, Texas

[17] American Standards for Testing and Materials, "Standard Test Methods for Chemical Analysis of Hydraulic Cement," ASTM International, ASTM C114-11, Annual Book of ASTM Standards

[18] East, B., "Laboratory and Field Investigations on the Use of Lithium Nitrate to Prevent or Mitigate Alkali-Silica Reaction," The University of Texas at Austin, Master's Thesis, 2007

[19] Bentivegna, A.F., "Development and Monitoring of an Outdoor Exposure Site to Mitigate Alkali-Silica Reaction in Hardened Concrete," The University of Texas at Austin, Master's Thesis, 2009

[20] Giannini, E.R., "Field Studies of Mitigation Strategies for Alkali-Silica Reaction in Hardened Concrete," The University of Texas at Austin, Master's Thesis

[21] Godart, B., Fasseu, P., Michel, M., "Diagnosis and Monitoring of Concrete Bridges Damaged by AAR in Northern France," Proceedings of the 9th International Conference on Alkali-Aggregate Reaction, London, Great Britain, July 1992, pp. 368-375.

TABLE 1: DRI features and weight factor.

Petrographic Feature Measured (Feature Name on DRI Summary Sheets)	**DRI Weight Factor**
Air voids with ASR gel	0.5
Cement paste with cracks and ASR gel	4
Cement paste with cracks	2
Reaction rim s around fine aggregate	0.25
Fine aggregate debonded	2
Fine aggregate with cracks and ASR gel	2
Fine aggregate with cracks	0.25
Reaction rim s around coarse aggregate	0.5
Coarse aggregate debonded	3
Coarse aggregate with cracks and ASR gel	2
Coarse aggregate with cracks	0.25

TABLE 2: Stiffness damage testing results.

Columns from North and South Loggia		
Element Location, Element Type, and Core No.	Energy Dissipated (J/m^3)	Accumulated Plastic Strain (μm/m)
SL-C-2	606.48	89.77
SL-C-3	801.78	96.06
SL-C-4	570.4	92.63
NL-C-2	704.32	88.18
NL-C-3	270.33	20.97
NL-C-4	401.53	43.39

Beams from North and South Loggia		
Element Location, Element Type, and Core No.	Energy Dissipated (J/m^3)	Accumulated Plastic Strain (μm/m)
SL-B-1.2	562.25	70.29
SL-B-2.3	679.50	77.40
NL-B-1.2	388.59	43.94
NL-B-2.3	413.45	54.90

TABLE 3: Residual expansion test results.

Columns from North and South Loggia	
Element Location, Element Type, and Core No.	Avg. Expansion, % (2 Cores)
SL-C-2	0.036%
SL-C-3	0.064%
SL-C-4	0.027%
NL-C-2	0.039%
NL-C-3	0.043%
NL-C-4	0.059%

Beams from North and South Loggia	
Element Location, Element Type, and Core No.	Avg. Expansion, % (2 Cores)
SL-B-1.2	0.035%
SL-B-2.3	0.024%
NL-B-1.2*	0.032%
NL-B-2.3**	N/A

* Due to the condition of the concrete only one core could be extracted from this location
** Due to the condition of concrete no cores could be successfully extracted from this location

TABLE 4: Hot-water extraction of water-soluble alkalis.

Columns from North and South Loggia	
Element Location, Element Type, and Core No.	Equivalent Na_2O_{eq} kg/m^3
SL-C-2	2.7
SL-C-3	3.0
SL-C-4	2.7
NL-C-2	4.0
NL-C-3	3.2
NL-C-4	3.4

Beams from North and South Loggia	
Element Location, Element Type, and Core No.	Equivalent Na_2O_{eq} kg/m^3
SL-B-1.2	3.0
SL-B-2.3	3.4
NL-B-1.2	2.3
NL-B-2.3	2.6

TABLE 5: Crack mapping index (CI) testing results.

Element Location, Element Type	# of Cracks	Total Crack Width (mm)	Average Crack Width (mm)	Average Crack width / m (mm)	Cracking Index (CI)
NL-C-2	40	9.4	0.24	2.76	2.7
NL-B-2.3	22	3.93	0.18	1.16	1.1
NL-C-4	44	12.24	0.28	3.60	3.6
SL-C-2	14	4.3	0.31	1.26	1.3
SL-C-2.3	26	6.6	0.25	1.94	1.9
SL-C-4	19	4.36	0.23	1.28	1.3

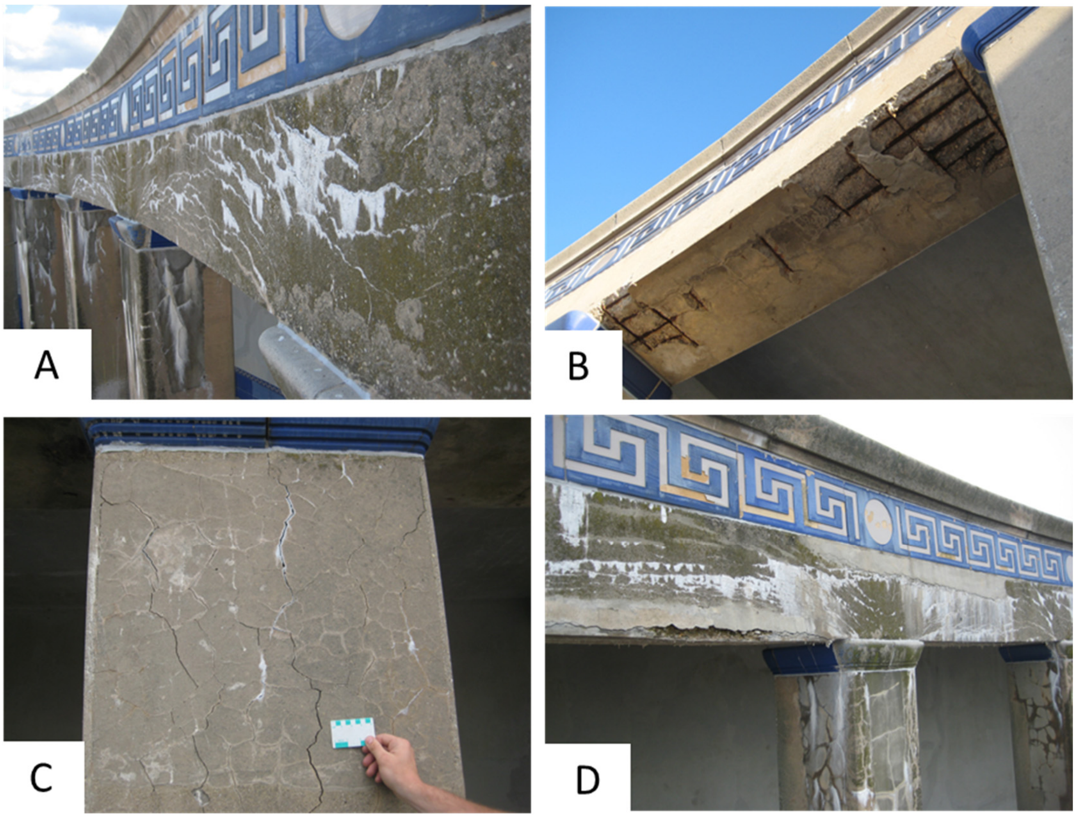

FIGURE 1: Typical existing conditions at OBBH A) cracking and efflorescence in beams and columns, B) spalling and corrosion of steel reinforcement, C) map pattern cracking in column, and D) cracking staining and efflorescence in beams and columns.

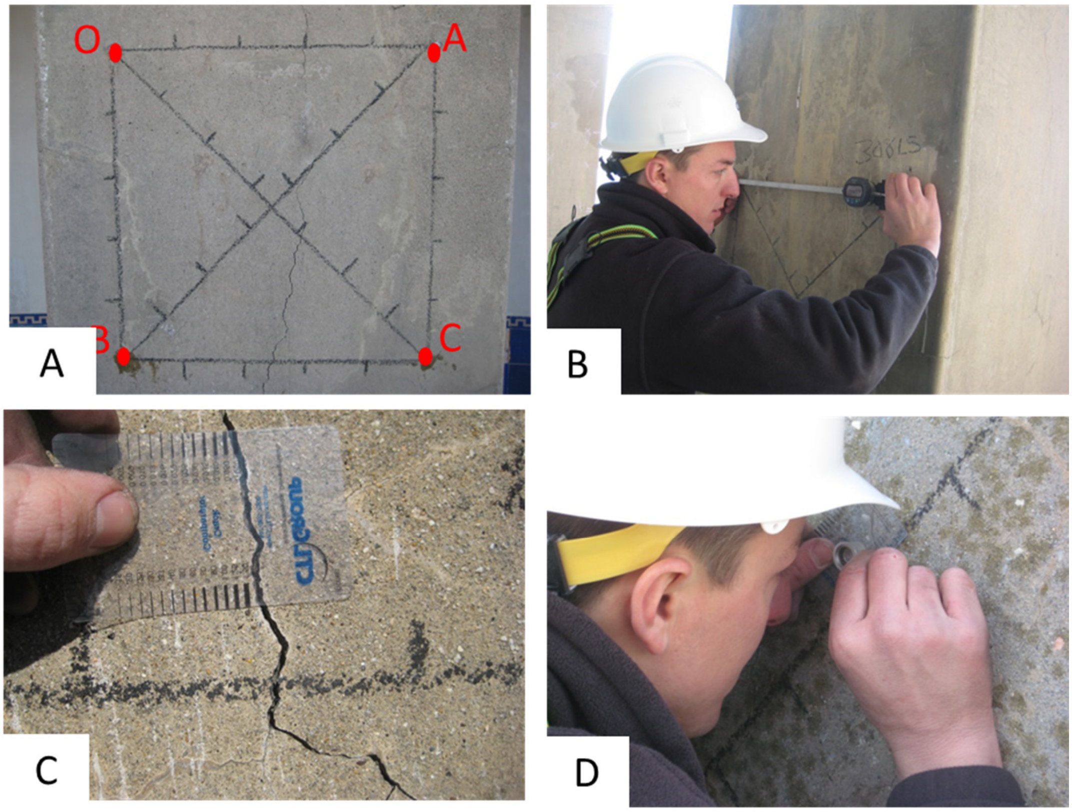

FIGURE 2: A) Gage pin layout, B) measuring the length between gage pins, C) crack propagation measurement pattern, and D) measuring crack widths.

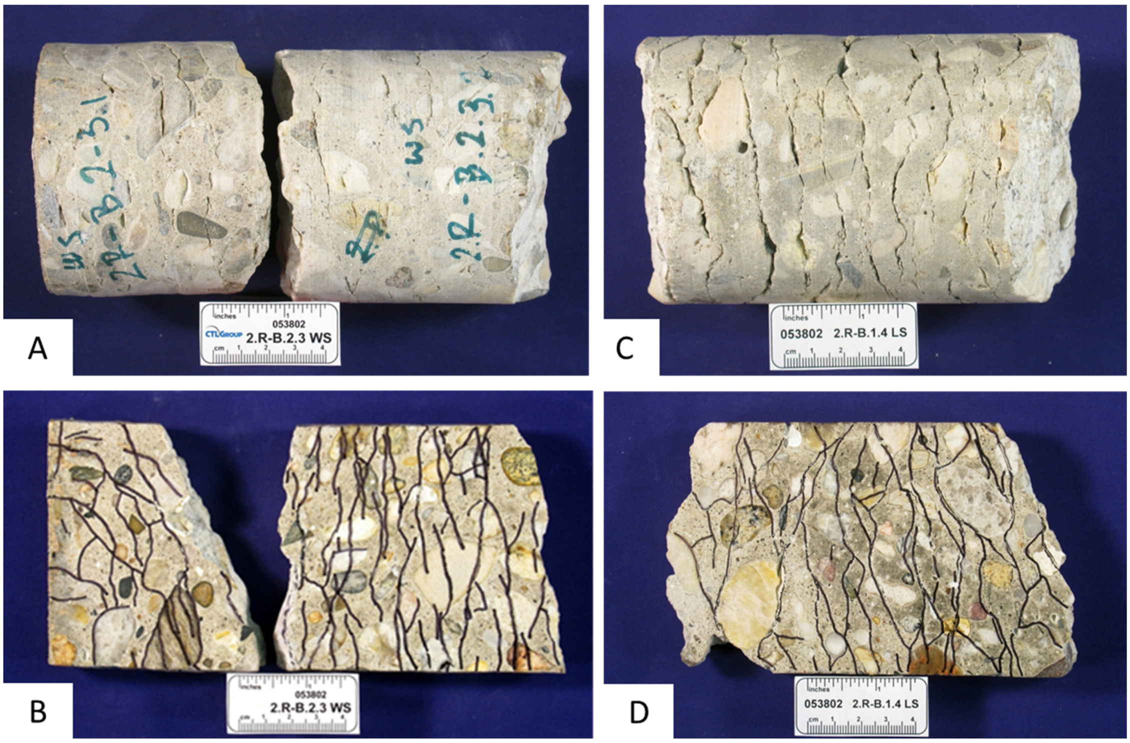

FIGURE 3: A) As-received photograph of core from loggia beam, B) lapped core with cracks highlighted with black marker, C) as-received photograph of core from loggia beam and D) lapped core with cracks highlighted with black marker.

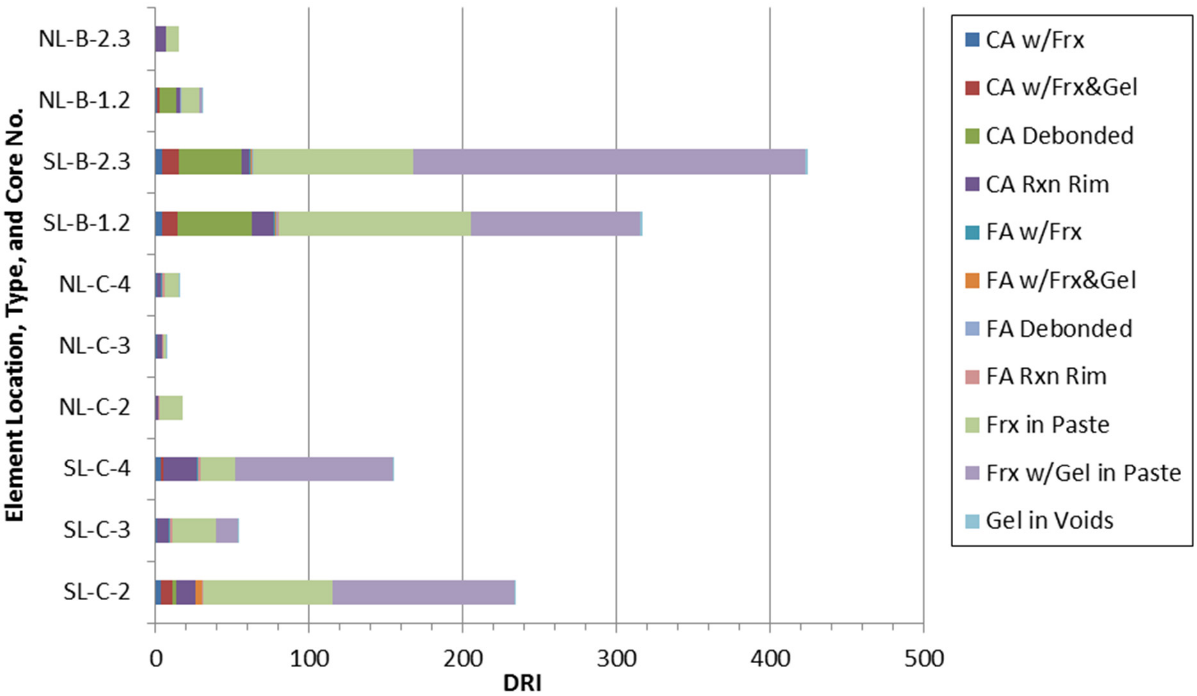

FIGURE 4: Results of the petrographic examination indicating the number of petrographic features for 100 cm² equivalent surface area.